Coupling mechanisms in exchange biased films (invited)

T. C. Schulthess[a] and W. H. Butler
Metals and Ceramics Division, Oak Ridge National Laboratory Oak Ridge, Tennessee 37831-6114

We use an atomistic Heisenberg model in conjunction with the classical Landau Lifshitz equation for the spin motion to study coupling mechanisms between ferromagnetic (FM) and antiferromagnetic (AFM) films. Calculations for CoO/FM illustrate that there are two coupling mechanisms at work, the spin–flop coupling and an AFM–FM coupling through uncompensated defects. While the latter accounts for exchange bias and related phenomena, the former gives rise to a large coercivity and perpendicular alignment between FM spins and AFM easy axis. A combination of the two mechanisms explains apparent discrepancies between reversible and irreversible measurements of the AFM–FM coupling. © *1999 American Institute of Physics.* [S0021-8979(99)31508-5]

I. THE PROBLEM OF AFM–FM COUPLING

''Exchange bias,'' [1] which refers to a shift (H_{eb}) in the magnetization curve away from the zero field axis, is probably the most intriguing of several phenomena[2] observed when a ferromagnet (FM) is in contact with an antiferromagnet (AFM). Consequently most theoretical work[1,3–9] on the subject has been primarily concerned with the description of this asymmetry in the magnetization curve. Despite four decades of research since its discovery, the understanding of this effect is still not established.

The key issue in a theory of exchange bias is understanding how the coupling between the AFM and FM leads to a *unidirectional* anisotropy. The experimentally observed shift in the magnetization curve implies that the two configurations at the respective endpoints of the curve have different energies. In the case of an AFM/FM system with large enough anisotropy in the AFM, only the spins in the FM will invert upon reversal of the applied field. Since the two configurations are not equivalent by inversion symmetry they can have different energies, depending on the nature of the coupling between the AFM and FM spins.

When the interfacial layer of the AFM is uncompensated and perfectly flat, the existence of a coupling between the FM and AFM is straightforward to understand.[1] It is clear that in a simple model in which the interfacial AFM spins maintain (approximately) their initial relative orientations, the initial and final configurations, before and after reversal of the applied field will have different energies. For this case, Neel[3] and later Mauri *et al.*[4] have shown, that realistic values for H_{eb} can be obtained when a domain wall forms in the AFM during the reversal of the FM magnetization. When the interface plane is compensated however, the nature of the AFM–FM coupling is not obvious.

Experiments indicate that the loop shift is of similar magnitude for compensated and uncompensated interfaces.[10,11] Furthermore, an interface which is, in principle, uncompensated at the atomic scale may be compensated on average over longer length scales when it is rough. Only when interfacial terraces are much larger than the AFM domain wall width, would one have the situation where the AFM can break up into domains which have uncompensated interfaces with the FM. Otherwise the AFM domains will span several terraces and their interface to the FM will be compensated. Thus the case of magnetically compensated AFM interface planes seems to be more relevant for the exchange bias problem.

Using localized atomic spins, Hinchey and Mills[12] and recently Koon[5] demonstrated that, due to frustration of interfacial spins, the FM magnetization will align perpendicular to the AFM easy axis when the AFM interface plane is compensated. This establishes the coupling between the FM and the AFM when the interface is compensated and is referred to as *spin–flop coupling*. However, contrary to Koon's expectation, spin–flop coupling does not lead to the formation of a domain wall in the AFM during FM magnetization reversal and therefore in itself does not lead to exchange bias.[13]

A different route was taken by Malozemoff,[6] who explained the coupling as due to a random field which he attributed to interface roughness. This theory is particularly appealing because it accounts for many of the observations that are related to the loop shift.[7] However, some of Malozemoff's conclusions with regard to dependence of the exchange bias on the AFM layer thickness[8] and the observed increase of H_{eb} with decreasing interface roughness in some systems[14] have led to arguments against his theory.[15,5] Suhl and Shuller[9] have recently proposed yet another mechanism which explains the loop shift. They use a quantum mechanical description of the spins and show that the emission and reabsorption of virtual spin waves leads to exchange bias.

Clearly there are several possible mechanisms that lead to the result that the energies of configurations with reversed FM magnetization are different which, in turn, implies a unidirectional shift of the magnetization curve. However, a theory has to explain other important effects that are known

[a]Electronic mail: schulthesstc@ornl.gov

 © 1999 American Institute of Physics

Downloaded 12 Mar 2002 to 128.219.47.178. Redistribution subject to AIP license or copyright, see http://ojps.aip.org/japo/japcr.jsp

to be related to the AFM–FM coupling. Discussing all of these effects would require ant entire book chapter. Thus we restrict ourselves to the following effects which have been observed in many different AFM–FM systems: (1) Exchange bias, positive and negative, as well as related phenomena discussed by Malozemoff[7] and the dependence of H_{eb} on the interface roughness. (2) The large coercivity[16–18] that is known to be related to the coupling because it disappears when the AFM is disordered. (3) The perpendicular alignment between the FM magnetization and the AFM easy axis.[16,17,19] (4) The observation that reversible measurements of the coupling can yield values several times larger than those determined from the loop shift, H_{eb}.[20,21]

While all of these effects are observed in some AFM/FM systems, some are missing in other systems. For example, a coercivity related to the coupling is observed when Permalloy (Py) is in contact with FeRh but the system shows no exchange bias.[18] The opposite is the case when FeMn or IrMn are used as AFMs: in these systems, the coercivity is small but the exchange bias can be considerable. The theory thus also has to be able to account for the possible absence of some of the effects.

In the present work, we start from a microscopic description within an extended Heisenberg model and use the Landau–Lifshitz equation to investigate the rather complex magnetic configurations that can occur at AFM–FM interfaces. We use CoO with (111) interface planes as a model AFM-layer, since it is the system for which many experiments are published and, more importantly, in which all of the above mentioned effects are observed. Our microscopic calculations will be limited to idealized situations in which the AFM and FM films are single crystals and in a single domain state (i.e., we exclude the formation of domain walls perpendicular to the interface). But nevertheless, we are able to show, that even in this simplified context most relevant effects can be accounted for. We will discuss implications of our results to situations that currently cannot be handled with a microscopic approach.

II. METHOD AND MODEL

In our model, a spin configuration is a set of three-dimensional vectors, $\mathbf{M}\equiv\{\vec{\mu}_i\}$, which are located on atomic sites, i where we assume the bilayer to be periodic in the two dimensions parallel to the interface. The energy of the spin configuration consists of four terms,

$$E[\mathbf{M}]=E_Z+E_J+E_A+E_D,$$

of which the first three are, respectively, the Zeeman energy, $E_Z=\Sigma_i\vec{\mu}_i\vec{H}_{\text{ext}}$, the exchange energy, $E_J=-\Sigma_{i\neq j}J_{ij}\vec{s}_i\vec{s}_j$, with $\vec{s}=\vec{\mu}/|\vec{\mu}|$, and the anisotropy energy, $E_A=\Sigma_i K_i\sin^2\theta_i$. The magnetic moments, μ_i, the exchange parameters, J_{ij}, and the anisotropy constants, K_i, for CoO/Py(111) and CoO/Co(111) bilayers have been specified elsewhere.[22] The mangnetostatic contribution to the energy is $E_D=\Sigma_{i\neq j}\{\vec{\mu}_i\vec{\mu}_j-3(\vec{\mu}_i\hat{n}_{ij})(\vec{\mu}_j\hat{n}_{ij})\}/|\vec{R}_i-\vec{R}_j|^3$, where $\hat{n}_{ij}$ is the unit vector that points into the direction that connect the sites at $\vec{R}_i$ and $\vec{R}_j$. The magnetic moments are subject to the Landau–Lifshitz equation of motion (EOM) with the Gilbert–Kelley form for the damping term,

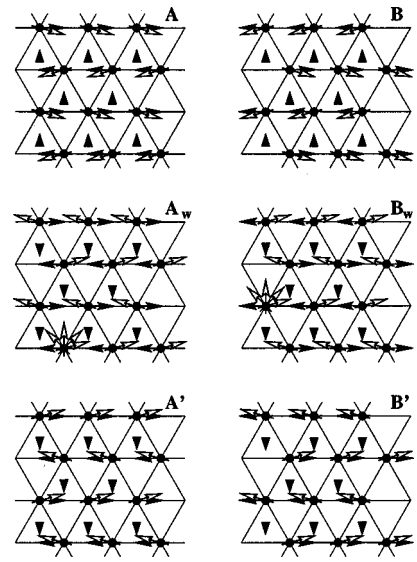

FIG. 1. Top view of CoO–FM (111) interface with compensated AFM interface plane. Filled and open arrows indicate, respectively, the unrelaxed and relaxed moment directions in the AFM layer. FM moment directions are given by triangles. The two possible spin-flop states for a given FM magnetization direction are labeled with **A** and **B**, respectively. $\mathbf{A_W}$ and $\mathbf{B_W}$ are the corresponding states with reversed FM magnetization and a domain wall in the AFM. The fan of arrows on one of the atoms indicates schematically how the moment directions change going into the AFM from the interfacial layer (open arrow) to the interior (filled arrow). The spin-flop states with reversed FM magnetization are denoted by $\mathbf{A}'$ and $\mathbf{B}'$.

$$\frac{\partial}{\partial t}\vec{\mu}_i=-\gamma(\vec{\mu}_i\wedge H_i)+\sigma\left(\vec{\mu}_i\wedge\frac{\partial}{\partial t}\vec{\mu}_i\right)\frac{1}{|\vec{\mu}_i|},$$

where $H_i[\mathbf{M}]=-(\partial/\partial\vec{\mu}_i)E[\mathbf{M}]$ is the local magnetic field, γ is the gyromagnetic ratio, and σ is an arbitrary damping parameter. The results do not depend on the actual values of the damping constant because the EOM is only used to find equilibrium solutions and to determine the stability of these solutions. With present computational resources, the treatment of domain walls perpendicular to the interface is not feasible with our method. We thus treat only states in which there is a single domain parallel to the interface in order that the magnetic configurations are two-dimensional periodic. This implies that during field reversal the magnetization rotates coherently. We start with an initial solution of the EOM for a certain applied field. Then we change the values of the applied field in steps and determine the new solution of the EOM. When the applied field is reversed and there is an energy barrier that prevents the FM from switching, the initial solution becomes metastable. By further increasing the magnitude of the field one approaches a bifurcation point where the metastable solutions becomes unstable and the FM magnetization switches to align with the applied field. The magnitude of the applied field at the bifurcation point then corresponds to the coercive field.

III. SPIN–FLOP COUPLING

We begin with a qualitative discussion of the possible spin configurations in our CoO/FM system. Since we assume the CoO interface plane to be compensated with a fixed uniaxial anisotropy, we are left with two equivalent AFM

Downloaded 12 Mar 2002 to 128.219.47.178. Redistribution subject to AIP license or copyright, see http://ojps.aip.org/japo/japcr.jsp

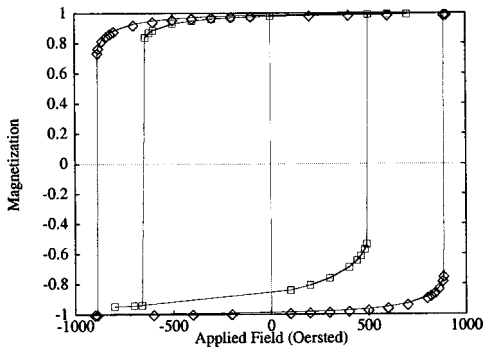

FIG. 2. Typical set of magnetization curves for perfect (diamonds) and rough (squares) interface. This particular example is for a 200 Å Py film with $J_{F-F}=16$ meV and AFM anisotropy axis along the $[\bar{1}\bar{1}7]$.

spin-configurations (denoted by **A** and **B** in Fig. 1). If both the AFM and the FM spins are rigidly aligned among themselves, the energy (with $H_{ext}=0$) is independent of the relative alignment between FM magnetization and AFM easy axis. However, when the spins are allowed to cant in order to minimize the energy (eg., by solving the EOM), the FM moments align perpendicular to the AFM easy axis which gives rise to the spin–flop coupling. In the following, we call the axis parallel to the interface and perpendicular to the AFM easy axis the *spin–flop coupling axis*.

For each AFM spin-configuration there are two ways to align the FM perpendicularly and we are left with four states (**A**, **A**′, **B**, and **B**′ in Fig. 1) that have the same energy when no external field is applied. The Zeeman term lifts the fourfold degeneracy when a field is applied and selects the two states which have an FM spin-component parallel to the field as the new energy minima. We choose the initial field directions such, that states **A** and **B** have lowest energy. Since both configurations are equivalent, we will choose **A** for the remainder of the discussion. When the magnetic field is reversed there are, in principle, two possible final configurations. The first possibility is the state in which a domain wall has formed in the AFM ($\mathbf{A_W}$ in Fig. 1). The second possibility is the spin-flop state with reversed FM spins (**A**′ in Fig. 1). Since, upon field reversal, configuration **A**′ is energetically equivalent to **A** the magnetization loop that corresponds to the path $\mathbf{A}\rightarrow\mathbf{A}'\rightarrow\mathbf{A}$ will not be shifted. On the other hand, $\mathbf{A_W}$ has to accommodate a domain wall and thus has higher energy than **A**′ and **A**. Therefore the loop of $\mathbf{A}\rightarrow\mathbf{A_W}\rightarrow\mathbf{A}$ will show exchange bias. This is as far as we can go with a qualitative discussion. The decision as to which of the two paths the spin-system follows depends on the relative energy barriers between the states and has to be determined numerically.

When the spin motion is restricted to the plane parallel to the interface, as in the calculation of Koon,[5] the path $\mathbf{A}\rightarrow\mathbf{A}'$ is impossible since it requires the spins to come out of plane when they rearrange. However, when the EOM is solved without any restriction,[13] the energy barrier of $\mathbf{A}\rightarrow\mathbf{A}'$ is lower than the domain wall energy in $\mathbf{A_W}$, and the system switches between **A** and **A**′ when the field is cycled, giving rise to a symmetric magnetization curve. This is the case in both models,[13] Koon's and the present CoO/FM bilayer. A typical magnetization curve is shown in Fig. 2. The effect of spin-flop is that it hinders the FM magnetization reversal giving rise to hysteresis with large coercivity. Values for H_c are given in Table I.

TABLE I. H_c for flat CoO/Py(200 Å) interface as well as H_c and H_{eb} for interface with uncompensated AFM-defects (in Oe).

AFM easy axis	J_{F-F} (meV)	Flat interface H_c	Interface with defects H_c	Interface with defects H_{eb}
$[\bar{1}\bar{1}7]$	16	885	575	75
$[\bar{1}01]$	16	1625	1250	74
$[\bar{1}01]$	9.4	1336	1039	38

IV. A MECHANISM FOR THE LOOP SHIFT

The conclusion of the last section is made under the idealized assumption that the interface is perfectly flat. Realistically, however, the interface will be rough and contain defects such as dislocations. A simplified way to incorporate defects related to interfacial roughness such as steps, islands, or point defects into our calculations, is to replace an FM site with a corresponding arrangement of AFM sites on the FM side of the interface. The case of a point defect is illustrated in Fig. 3. The defect moment is coupled to only one of the two AFM sublattices. The net interaction of the FM with the two AFM sublattices is no longer balanced. This causes the FM to cant away from the spin–flop coupling axis as indicated by configuration **D** in Fig. 3. Configuration **D** is only one of four possible states with lowest energy, and we assume that it was selected by an external field that points into the second quadrant of the *xy* plane. When the field and the FM magnetization are reversed we arrive at configuration **D**′ in Fig. 3. As a consequence of the unbalanced exchange coupling between the FM, the defect and the AFM, the energy of **D**′ will be higher and the magnetization curve that corresponds to $\mathbf{D}\rightarrow\mathbf{D}'\rightarrow\mathbf{D}$ will be shifted.

The magnitude of the shift depends on the density of these uncompensated defects (larger shift for more uncompensated defects). For CoO/Py, however, Takano *et al.*[23] have measured the amount of uncompensated AFM magnetization along the direction of the applied field and have shown that it correlates with the values of H_{eb}. In our calculation, we use a 4×4 unit cell with one point defect per cell and apply a field parallel to the interface plane at an

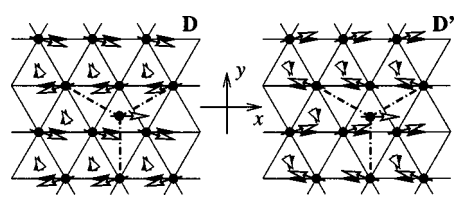

FIG. 3. Magnetic configuration of an CoO–FM (111) interface, where one FM site has been replaced by an AFM site. The nomenclature is similar to that of Fig. 1, where the open triangles in configuration **D** indicate that the FM moments are slightly canted away from the ideal spin–flop coupling axis. In configuration **D**′ the FM spins are simply inverted. Dashed lines highlight the next nearest neighbor interactions between the defect site and one of the two AFM sublattices.

Downloaded 12 Mar 2002 to 128.219.47.178. Redistribution subject to AIP license or copyright, see http://ojps.aip.org/japo/japcr.jsp

angle $\phi_H = 10°$ from the y axis. For this setup, we find that the amount of uncompensated AFM magnetization projected onto the field axis is about 1% of the moments in a CoO monolayer. For this amount and a Py film thickness of $d_{FM} = 300$ Å Takano *et al.* measured a loop shift of 50 Oe (this corresponds to about 75 Oe when $d_{FM} = 200$ Å). A typical magnetization curve is shown in Fig. 2 and the calculated loop shifts and coercivities are given in Table I. The calculated values for H_{eb} agree reasonably well with experiment.

We conclude this section with a remark on positive exchange bias. In configuration **D**, the net uncompensated AFM magnetization points away from the FM spins and the applied field. This is because the negative exchange coupling to the FM overwhelms the Zeeman coupling between the net magnetization of the defect and the applied field. In principle, however, one could think of a different system in which the Zeeman coupling of the defect is more important for very large cooling fields. In this case the spin-configuration is preset into the state with higher energy (which corresponds to $\mathbf{D}'$) and would switch to the lower energy state upon field reversal, resulting in a positive shift of the magnetization curve. Note that cooling in a very large field is the actual requirement to observe positive exchange bias.[24]

V. REVERSIBLE MEASUREMENTS

In order to determine the spin–flop coupling strength, we apply a small field, $H_\perp$, parallel to the interface plane but perpendicular to the spin–flop coupling axis ($\phi_H = 90°$). We then solve the EOM and determine the energy difference $\Delta E = E(H_\perp) - E(0)$ and the angle, ϕ, between the total magnetization and the coupling axis. For small enough fields[25] the results satisfy the relations

$$\Delta E = K_{eff}(d_{FM}) \sin^2 \phi \approx K_{eff}(d_{FM}) \phi^2, \tag{1}$$

where we have introduced effective coupling strength, K_{eff}. Since the spin–flop coupling only applies to interfacial spins and the FM spins are not rigidly coupled to each other, the FM magnetization will twist when the field $H_\perp$ is applied. The energy of this twist is contained in ΔE and depends on the thickness, d_{FM}, of the FM film. Thus K_{eff} shows a thickness dependence as well. Coupling the FM spins rigidly to each other would remedy this problem but would also change the spin–flop coupling strength, since the spin-relaxation in the FM also contributes to the effective coupling. Our method for calculating K_{eff} is equivalent to the experiment of Miller and Dahlberg,[20] who have applied a small field perpendicular to the Co magnetization in a CoO/Co bilayer and determined the angle ϕ with the anisotropic magneto-resistance technique. The theoretical and experimental coupling constants are compared in Fig. 4 where the difference in the definition of the coupling constants between our and the experimental work[20] requires the inclusion of the factor 2. The agreement between the calculated and the experimental results is remarkable, particularly since we have not adjusted any parameters. The quantitative agreement should, however, not be overstated since the model of the bilayer and the Heisenberg Hamiltonian used for the calculation both contain significant approximations.

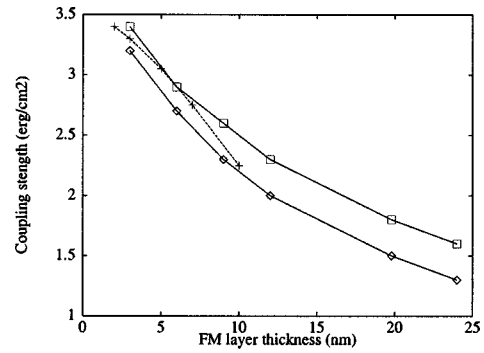

FIG. 4. Effective AFM–FM coupling strength between CoO and Co vs thickness of the Co film. Experimental values (crosses) are taken from Ref. 20. Theoretical values represent $2K_{eff}$ calculated for $J_{F-F} = 16$ meV (squares) and $J_{F-F} = 12.4$ meV (diamonds).

VI. DISCUSSION

In the previous three sections we have shown that the perpendicular coupling, the coercivity, the loop shift, and the strong coupling seen in reversible measurements, can be understood within an atomistic Heisenberg model. The model used in the calculations, however, is in many respects too simple to accurately describe the situation in thin films. It envisions a periodic arrangement of one type of defect and gives the proper loop shift, but it does not explain other effects related to the loop shift. In a realistic interface, the defects will be of different types and will be randomly arranged. On average, the interactions between the AFM and the FM may be fully compensated when the AFM is in a single domain state. However, when the system is cooled in the presence of coupling to an ordered FM film, the AFM may break up into domains with walls perpendicular to the interface such that the exchange coupling due to the defects no longer cancels. This is precisely the mechanism that leads to the Imry–Ma type of random field.[26] Therefore, extending the current model of rough interfaces to realistic length scales leads directly to the Malozemoff theory of exchange bias which accounts for many of the effects related to the loop shift.[7] The explanation of positive exchange bias which we have given at the end of Sec. IV is still applicable within the random field model. To complete the list of effects related to the loop shift, we have to discuss the dependence of H_{eb} on the roughness. Experiments show that interface roughness can both increase[27] or decrease[14] the loop shift. Clearly, when the random field is solely due to roughness induced defects, such as the point defects treated in Sec. IV, one would expect the random field and with it H_{eb} to increase with increasing roughness. However, when the random field is induced by uncompensated regions that are related to lattice strain (such as dislocations) one would observe the opposite trend: since roughness decreases lattice strains it would lower the random field and H_{eb}.

In thin films, the magnetization reversal is usually not a coherent rotation as in our calculations. Reversal is rather initiated in some region of the film and is completed through

Downloaded 12 Mar 2002 to 128.219.47.178. Redistribution subject to AIP license or copyright, see http://ojps.aip.org/japo/japcr.jsp

growth of reversed domains, a process which implies the propagation of domain walls through the film. Spin–flop coupling can now lead to an increase in the coercivity in two different ways. First, some of the AFM domains, to which the FM couples, are small enough that their magnetic configuration reverses during the inversion of the FM. This leads to irreversible effects in the AFM that contribute to the coercivity. This idea was used by Lin *et al.*[28] and recently by Stiles and McMichael,[29] as well as by Hou *et al.*[30] to explain irreversible effects in polycrystalline AFM/FM systems.

In a second mechanism, spin–flop coupling acts like an induced uniaxial anisotropy in the FM layer which reduces the size of domain walls when the FM is coupled to the AFM and thus increases the coercivity through pinning of these domain walls. In free Py the anisotropy is very small ($K_{\mathrm{Py}} \simeq 20\times 10^3\ \mathrm{erg/cm^3}$) which implies large domain walls for which pinning is very unlikely and consequently the material is magnetically ideally soft. When the AFM–FM coupling is averaged over the entire film thickness, our results in the previous section would yield a uniaxial anisotropy of the order of $0.5\times 10^6\ \mathrm{erg/cm^3}$ for a 200 Å thick-film, which is comparable to anisotropies in Fe. Spin–flop coupling, however, is due to relaxation of spins in the interface region and the anisotropy it induces is therefore concentrated in that region. Assuming this region to be about 10 Å and a corresponding estimate for the coupling of $K_{\mathrm{eff}} \approx 2\ \mathrm{erg/cm^2}$, one is left with an average anisotropy constant of about $2\times 10^7\ \mathrm{erg/cm^3}$ which is about three order of magnitude larger than the bulk value for Py. The domain wall size in the film can thus be expected to reduce from $\sim 10^3$ Å to below 100 Å and pinning of domain walls in Py would then be realistic when the film is coupled to an AFM such as CoO.

These two mechanisms for the coercivity have quite distinct consequences. In the first mechanism, the coercivity depends on the domain structure in the AFM and therefore can be expected to depend on the magnetic history of the sample. In the second mechanism, the coercivity only depends on the spin–flop coupling and the morphology of the film. It is not affected by the AFM domain structure and thus should be independent of the magnetic history.

Since exchange bias and the coupling induced coercivity have their origin at the interface, one expects them to be inversely proportional to the thickness of the FM layer. For the loop shift this is well accepted. In the case of the coercivity, however, this is only a first guess which may apply when the coercivity is due to losses in the AFM. If it is due to the coupling induced reduction of domain walls discussed above, the functional dependence of domain wall size and defect densities at different length scales have to be considered as well. The size of a domain wall depends not only on the anisotropy, which in the present case is restricted to the interface region and has no dependence on d_{FM}, but also on the exchange interactions. The net FM exchange energy of a domain wall in the film increases linearly with the film thickness, which implies that the domain wall size will be proportional to $\sqrt{d_{\mathrm{FM}}}$. The density of defects which pin the wall is more difficult to discuss and we will restrict ourselves to two model situations. (1) When the defect density is constant at all length scales below a certain threshold, the pinning will be independent of the domain wall size as long as it is small enough. In this case one expects $H_c \sim 1/d_{\mathrm{FM}}$. (2) We assume that the interface is of fractal nature and when the domain wall size, d_w, is decreased, the density of defects that can pin the wall increases as $1/d_w$. With $d_w \sim \sqrt{d_{\mathrm{FM}}}$, we thus expect $H_c \sim 1/d_{\mathrm{FM}}^{3/2}$. This last result is similar to that recently obtained by Zhang.[31]

In contrast to the irreversible process of magnetization reversal, the reversible measurements of Miller and Dahlberg[20] are much simpler to model. Actually, we think that the calculations presented in the last section fully correspond to this measurement and thus it does not need further explanation. The combination of spin–flop coupling and defect induced random field, however, clarifies the apparent discrepancy between reversible and irreversible measurement. While the former senses a (not necessarily linear) superposition of random field and spin–flop coupling, the latter only measures the coupling due to the random field.

VII. CONCLUSIONS

We can therefore conclude that two coupling mechanisms, spin–flop coupling and defect induced random fields, must be present, in order to explain all four classes of phenomena which are directly related to AFM–FM coupling. The consequences of the possible absence of one of the mechanisms are relatively straightforward. The absence of uncompensated defects and the corresponding random field would eliminate the loop shift, but if spin–flop coupling were still present, one should still be able to measure strong coupling in reversible experiments, observe coupling induced coercivities, and the perpendicular coupling. On the other hand, if spin–flop coupling were absent while the defect induced random field is present, the system would show exchange bias but no coupling induced coercivity. In this case, perpendicular coupling would not be observable but more importantly, the results of reversible and irreversible coupling measurement should be similar.[32]

When we apply these conclusions to Py interfaced with either NiMn, FeRh, and FeMn or IrMn, we argue that both coupling mechanisms are present in NiMn/Py whereas in FeRh/Py, the random field should be absent but spin–flop coupling should be considerable. Thus in both systems one should observe strong coupling in reversible measurements and perpendicular alignment between the FM magnetization and the AFM easy axis. In FeMn/Py and IrMn/Py, we speculate that the random field is present but the spin–flop coupling is much smaller since the coupling induced coercivity is much smaller. In fact, the discrepancy between irreversible and reversible coupling measurements in IrMn/Py is found to be at least an order of magnitude smaller than in NiMn/Py.[21] The spin–flop coupling strength seems to be related to the AFM spin-structure of these alloys. NiMn and FeRh with large spin–flop coupling are chemically ordered systems with collinear spin structures[33,34] and thus the situation is similar to that of CoO. FeMn and IrMn, for which the current discussion implies much smaller spin–flop coupling are chemically disordered and probably have noncollinear spin structures[35] which may cause the reduction in spin–flop cou-

Downloaded 12 Mar 2002 to 128.219.47.178. Redistribution subject to AIP license or copyright, see http://ojps.aip.org/japo/japcr.jsp

pling strength. The absence of exchange bias in FeRh/Py is not only intriguing but, in our opinion, implies a great opportunity, since comparing interfacial spin structures and morphologies between NiMn/Py and FeRh/Py could give important information on defect induced coupling and random fields.

ACKNOWLEDGMENTS

Research sponsored by the Division of Materials Sciences, U.S. Department of Energy under Contract No. DE-AC05-96OR22464 with Lockheed Martin Energy Research Corporation.

[1] W. H. Meiklejohn and C. P. Bean, Phys. Rev. **105**, 904 (1957).
[2] J. Nogués and Ivan K. Schuller, J. Magn. Magn. Mater. (in press).
[3] L. Neél, Ann. Phys. (Paris) **2**, 61 (1967).
[4] D. Mauri, H. C. Siegmann, P. S. Bagus, and E. Kay, J. Appl. Phys. **62**, 3047 (1987).
[5] N. C. Koon, Phys. Rev. Lett. **78**, 4865 (1997).
[6] A. P. Malozemoff, Phys. Rev. B **35**, 3679 (1987).
[7] A. P. Malozemoff, J. Appl. Phys. **63**, 3874 (1988).
[8] A. P. Malozemoff, Phys. Rev. B **37**, 7673 (1988).
[9] H. Suhl and I. K. Schuller, Phys. Rev. B **58**, 258 (1998).
[10] R. Junblut *et al.*, J. Magn. Magn. Mater. **148**, 300 (1995).
[11] J. Nogués, D. Lederman, T. J. Moran, Ivan K. Schuller, and K. V. Rao, Appl. Phys. Lett. **68**, 3186 (1996).
[12] L. L. Hinchey and D. L. Mills, Phys. Rev. B **34**, 1689 (1986).
[13] T. C. Schulthess and W. H. Butler, Phys. Rev. Lett. **81**, 4516 (1998).
[14] J. Nogués, D. Lederman, T. J. Moran, I. K. Schuller, and K. V. Rao, Appl. Phys. Lett. **68**, 3186 (1996).
[15] P. J. van der Zaag, A. R. Ball, L. F. Feiner, R. M. Wolf, and P. A. A. van der Heijden, J. Appl. Phys. **79**, 5103 (1996).
[16] T. J. Moran and I. K. Schuller, J. Appl. Phys. **79**, 5109 (1996).
[17] Y. Ijiri, J. A. Borchers, R. W. Erwin, S.-H. Lee, P. J. van der Zaag, and R. M. Wolf, Phys. Rev. Lett. **80**, 608 (1998).
[18] S. Yuasa, M. Nývlt, T. Katayama, and Y. Suzuki, J. Appl. Phys. **83**, 6813 (1998).
[19] T. J. Moran, J. Nogués, D. Lederman, and I. K. Schuller, Appl. Phys. Lett. **72**, 617 (1998).
[20] B. H. Miller and E. Dan Dahlberg, Appl. Phys. Lett. **69**, 3932 (1996).
[21] T. G. Pokhil and S. Mao (unpublished).
[22] See Ref. 13 for details about the model and parameters. In the present work, we do not vary the AFM–FM exchange parameter but rather fix it to the values of the exchange in the AFM. Whenever the value for the FM–FM exchange parameter, $J_{\mathrm{F-F}}$, differs from Ref. 13 as is mentioned in the text.
[23] K. Takano, R. H. Kodama, A. E. Berkowitz, W. Cao, and G. Thomas, Phys. Rev. Lett. **79**, 1130 (1997).
[24] J. Nogués, D. Lederman, T. J. Moran, and I. K. Schuller, Phys. Rev. Lett. **76**, 4624 (1996).
[25] For field larger than a few hundred Oersted, the induced changes in the AFM become notable and change the form of the field dependence of the total energy.
[26] Y. Imry and S.-K. Ma, Phys. Rev. Lett. **35**, 1399 (1975).
[27] T. J. Moran, J. M. Gallego, and I. K. Schuller, J. Appl. Phys. **78**, 1887 (1995).
[28] T. Lin, C. Tsang, R. E. Fontana, and J. Kent Howard, IEEE Trans. Magn. **31**, 2585 (1995).
[29] M. Stiles and R. D. McMichael, Phys. Rev. B (in press).
[30] C. Hou, H. Fujiwara, F. Ueda, and H. S. Cho, Mater. Res. Soc. Symp. Proc. (to be published).
[31] S. Zhang, J. Magn. Magn. Matter (in press).
[32] We assume that all effects are related solemnly to the AFM–FM coupling. FeF_2/Fe is a system in which, as Moran *et al.*[19] pointed out, perpendicular alignment could be related to lattice strain.
[33] T. C. Schulthess and W. H. Butler, J. Appl. Phys. **93**, 7225 (1998).
[34] V. L. Moruzzi and P. M. Marcus, Phys. Rev. B **48**, 16106 (1993).
[35] T. C. Schulthess, W. H. Butler, G. M. Stocks, S. Maat, and G. J. Mankey (unpublished).

Downloaded 12 Mar 2002 to 128.219.47.178. Redistribution subject to AIP license or copyright, see http://ojps.aip.org/japo/japcr.jsp